Urethane cross-linked poly(oxyethylene)/siliceous nanohybrids doped with Eu3+ ions - Part 2. Ionic association

ARTICLE *in* PHYSICAL CHEMISTRY CHEMICAL PHYSICS · JANUARY 2004

Impact Factor: 4.49 · DOI: 10.1039/b308202d

RESEARCH PAPER

PCCP
www.rsc.org/pccp

Urethane cross-linked poly(oxyethylene)/siliceous nanohybrids doped with Eu^{3+} ions

Part 2.† Ionic association

Verónica de Zea Bermudez,*[a] Denis Ostrovskii,[b] Sergei Lavoryk,[b] M. Cristina Gonçalves[a] and Luís D. Carlos[c]

[a] *Departamento de Química and CQ-VR, Universidade de Trás-os-Montes e Alto Douro, 5001-911 Vila Real, Portugal. E-mail: vbermude@utad.pt; Fax: 00-351-259-350480; Tel: 00-351-259-350253*

[b] *Department of Experimental Physics, Chalmers University of Technology, 41296, Göteborg, Sweden*

[c] *Departamento de Física and CICECO, Universidade de Aveiro, 3810-193, Aveiro, Portugal*

Received 17th July 2003, Accepted 5th December 2003
First published as an Advance Article on the web 12th January 2004

Fourier transform mid-IR and Raman spectroscopies were employed to investigate the anionic local surrounding in sol–gel derived organic/inorganic materials–*monourethanesils*–incorporating europium triflate, $Eu(CF_3SO_3)_3$. The hybrid framework of these xerogels contains short methyl end capped polyether segments grafted to a siliceous network through urethane cross-links. Samples with compositions $\infty > n \geq 10$ (where n indicates the ratio of (OCH_2CH_2) moieties per lanthanide ion) were examined. The spectral data obtained provide conclusive evidence of the presence of "free" and weakly coordinated $CF_3SO_3^-$ ions located in two distinct sites in the whole range of salt concentration analyzed. At $n = 30$ and 10, along with these species, two new anionic configurations, assigned to contact ion pairs and "cross-link separated" ions pairs, emerge. Two-dimensional correlation spectroscopic analysis allowed to clarify the number of components present in two critical bands containing strongly overlapped spectral profiles. The number of anionic environments found in the m-Ut(750)$_n$Eu$(CF_3SO_3)_3$ family confirms the rich coordinating possibilities offered by polymer systems incorporating trivalent triflate salts.

Introduction

This paper is the second of two papers devoted to the investigation of a family of Eu^{3+}-based sol–gel derived organic/inorganic materials designated as *monourethanesils*.[1–3] These xerogels were recently introduced with the goal of serving as model compounds of a series of structurally complex poly(oxyethylene), POE/siloxane hybrids (*diureasils*)[4] that are excellent candidates for the construction of new low cost, multipurpose, one material-based devices, combining several technologically useful features, such as, for instance, conducting, optical and magnetic properties.[4–7]

With the scope of gaining a deeper knowledge of the structure/properties relationship in the diureasil system, we will continue to examine in the present work the same set of europium triflate, $Eu(CF_3SO_3)_3$-doped *monourethanesil* samples analyzed in Part 1.[3] The compounds studied include short methyl end capped POE chains covalently bonded to a siliceous backbone through urethane groups. The host matrix was termed m-Ut(750), where m stands for mono, Ut indicates the urethane linkage and 750 denotes the average molecular weight of the organic precursor used (corresponding to about 17 (OCH_2CH_2) repeat units).

In Part 1, Fourier transform mid-IR (FT-IR) and Raman (FT-Raman) spectroscopies, photoluminescence spectroscopy and differential scanning calorimetry enabled us to conclude that, in terms of cation/polymer and cation/cross-link interactions, the m-Ut(750)-based xerogels may be viewed as an adequate replica of the long-chain U(2000)$_n$Eu$(CF_3SO_3)_3$ diureasil parent analogs (where U indicates the urea group, 2000 denotes the average molecular weight of the organic precursor used and n is the ratio of (OCH_2CH_2) units per Eu^{3+} ion).[3]

As the role of the anion on the coordination of the Eu^{3+} ions in the monourethanesil-type system has not been considered yet, we will be specifically concerned in Part 2 with the evaluation of the extent of ionic association in the m-Ut(750)$_n$-Eu$(CF_3SO_3)_3$ nanocomposites in order to shed more light into the description of the local chemical environment of the lanthanide ions which was initiated in Part 1.[3]

The $Eu^{3+}\cdots CF_3SO_3^-$ interactions in the m-Ut(750)$_n$-Eu$(CF_3SO_3)_3$ hybrids will be assessed through a FT-IR/FT-Raman spectroscopic analysis of the characteristic modes of the $CF_3SO_3^-$ ion. This anion is an excellent probe for investigating the cationic and anionic environments in salt/polymer systems, since the assignment of its internal vibration modes is well established.[8,9] The differentiation between the various associated species (contact ion pairs, solvent separated ion pairs, ionic multiplets or salt aggregates) is manifested in the spectra through different frequency shifts and/or splittings of different magnitude of characteristic vibrational bands of the "free" anion.[8–21]

The present spectroscopic analysis will essentially rely on deconvolution procedures. Unfortunately, the curve-fitting of some of the triflate bands which are most sensitive to coordination effects is not straightforward, as they are in general broad and commonly contain multiply overlapped components. To unravel the most critical triflate regions of the spectra of the monourethanesils, we will also employ two-dimensional (2D) correlation spectroscopic analysis.[22]

† For Part 1 see preceding paper (ref. 3).

DOI: 10.1039/b308202d

Results and discussion

1 IR and Raman spectroscopic data

It is generally assumed that a "free" $CF_3SO_3^-$ ion in a staggered configuration with a C_{3v} point group symmetry possesses 18 normal modes with the symmetry representations $5A_1 + A_2 + 6E$. The A_1 and E modes are IR and Raman active, whereas the A_2 mode, associated with the internal torsion of the anion, is inactive both in IR and Raman. All these modes are to a greater or lesser extent sensitive to coordination effects and can thus be employed to probe the local chemical surrounding experienced by the anion.[8–21]

The characteristic bands of the $CF_3SO_3^-$ ion are clearly discerned in the room-temperature FT-IR spectra of the m-Ut(750)$_n$Eu$(CF_3SO_3)_3$ monourethanesils between 1400 and 550 cm^{-1} (Fig. 1) and in the room-temperature FT-Raman spectra of the same compounds in the 1600–100 cm^{-1} spectral range (Fig. 2). Their frequency and assignment are given in Table 1. The specific spectral behavior of the xerogels investigated in the present work as a function of salt content will be discussed in detail below.

$\nu_a(SO_3)$ region. The FT-IR spectra of the m-Ut(750)-based compounds with $400 \geq n \geq 30$ exhibit a broad envelope in the $\nu_a(SO_3)$ region (Fig. 1). On the contrary, the FT-IR spectrum of the m-Ut(750)$_{10}$Eu$(CF_3SO_3)_3$ hybrid displays a series of sharp, distinct bands centered at about 1317, 1293, 1284, 1273, 1252 and 1216 cm^{-1} (Fig. 1).

Close analysis of the FT-IR spectrum of the non-doped hybrid host represented in Fig. 1 reveals that between 1350 and 1200 cm^{-1} the contribution of the polymer vibration modes is quite strong, a fact that complicates the detection of the triflate bands in the spectra of the materials incorporating Eu^{3+} ions. In order to discriminate the spectral changes introduced by the addition of $Eu(CF_3SO_3)_3$ to m-Ut(750), we will examine the FT-IR difference spectra reproduced in Fig. 3. These curves were obtained by subtracting the spectrum of the non-doped matrix from those of the salt containing xerogel materials with $n > 10$. This approach was not applied, however, to the m-Ut(750)$_{10}$Eu$(CF_3SO_3)_3$ sample because in this compound, unlike in the more dilute monourethanesils, the polyether segments play an active role in the coordination of the lanthanide ions, that results in dramatic morphological modifications in the polymer chains (Fig. 1 and Part 1[3]). Fig. 3 allows to infer that in the $\nu_a(SO_3)$ region the most pronounced effect originating from the addition of increasing amounts of the guest lanthanide salt is the growth of a wide structured feature centered around 1274 cm^{-1}. The inset in Fig. 3 shows that this band can be resolved into three components centered at about 1287, 1274 and 1262 cm^{-1} (Table 1). The typical results of the curve-fitting carried out in this envelope for the xerogel with $n = 70$ are reproduced in Fig. 4. Fig. 3 also demonstrates that the band shape of the $\nu_a(SO_3)$ event remains practically unchanged for a wide range of salt concentration ($400 \geq n \geq 50$), meaning that the increase of the guest salt content within this composition range does not change the general picture of the cation–anion interactions in the system.

Fig. 1 substantiates that, in the $\nu_a(SO_3)$ region, the band contour of the rich-salt m-Ut(750)-based composite with $n = 10$ is drastically different from those of the monourethanesils with $400 \geq n \geq 50$. The tremendous spectral modifications discerned in this spectrum start to develop already in that of

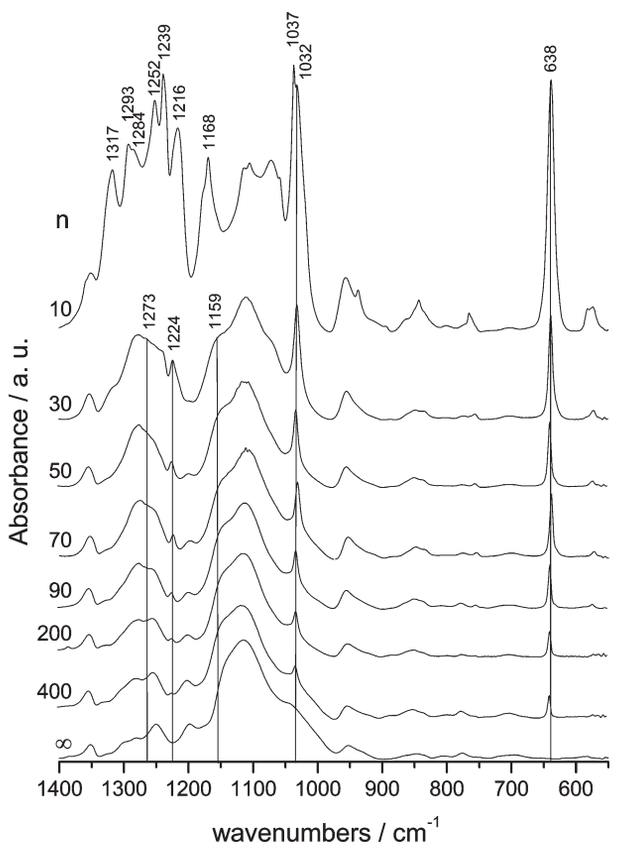

Fig. 1 Room-temperature FT-IR spectra of the m-Ut(750)$_n$-Eu$(CF_3SO_3)_3$ monourethanesils in the 1400–550 cm^{-1} region. The spectra have been scaled so that the height of the νCH_2 band is approximately the same.

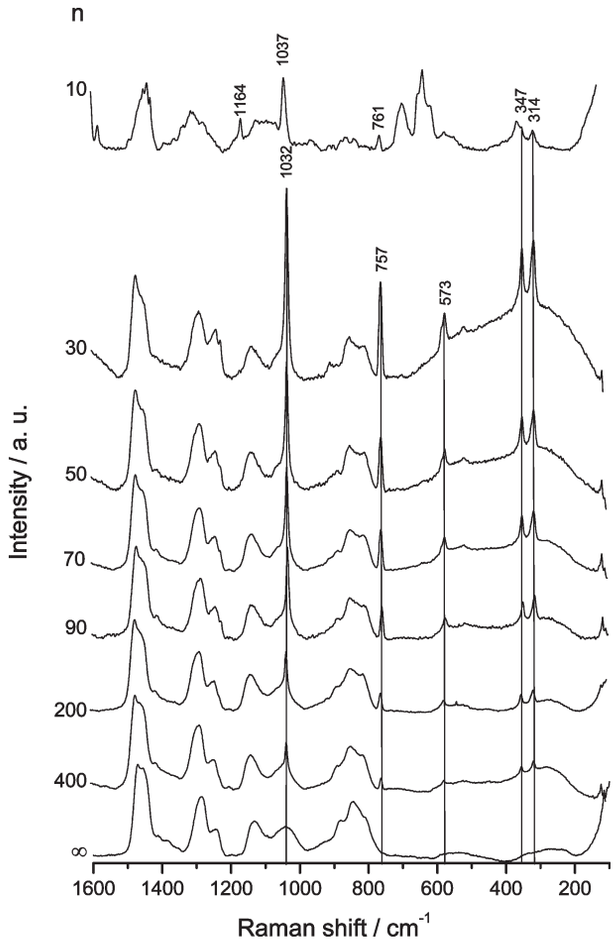

Fig. 2 Room-temperature FT-Raman spectra of the m-Ut(750)$_n$-Eu$(CF_3SO_3)_3$ monourethanesils in the 1600–100 cm^{-1} region. The spectra have been scaled so that the height of the νCH_2 band is approximately the same.

Table 1 Characteristic triflate bands of the FT-IR and FT-Raman spectra of the m-Ut(750)$_n$Eu(CF_3SO_3)$_3$ monourethanesils

m-Ut(750)$_n$Eu(CF_3SO_3)$_3$														POE$_n$Eu(CF_3SO_3)$_3$				
400		200		90		70		50		30		10		16[20a]			40[19b]	
IR	R	IR	R	IR	R	IR	R	IR	R	IR	R	IR	R	IR	R	$CF_3SO_3^-$[9]	Attribution	
										1316 sh		1317 s		1322			$\nu_a(SO_3)$	Contact ion pairs
										1297 sh		1295 s						"Cross-link separated ion pairs"
		1288 sh		1288 sh		1287 sh		1286 sh		1287 sh		1284 S						Weakly coord. anion
		1274 m		1274 m		1274 m		1273 S		1274 S		1274 sh		1272		1273		Free anion
		1261 sh		1262 sh		1263 m		1261 sh		1263 s		1262 sh						Weakly coord. anion
										1251 s		1251 s						"cross-link separated ion pairs"
		1234 sh		1236 sh		1233 sh		1235 sh		1237 s		1237 vs		1236			$\nu_s(CF_3)$	Coord. anion
		1222 m		1223 m		1223 m		1223 m		1223 m		1224 sh				1222		Free anion
		1212 sh		1213 sh		1215 sh		1213 sh		1213 sh		1213 s		1211			$\nu_a(SO_3)$	Contact ion pairs
												1186 sh					$\nu_a(CF_3)$	Coord. anion
												1178 sh						Coord. anion
										1171 sh		1170 vs						Coord. anion
												1164 sh						Coord. anion
1154 sh		1155 sh		1157 sh		1158 sh		1158 sh		1158 sh		1156 sh				1157[8]		Free anion
												1042 sh	1045 sh				$\nu_s(SO_3)$	Cryst. complex
1040 sh	1037 sh	1038 sh	1040 sh	1039 sh	1039 sh	1040 sh	1036 sh	1039 sh	1039 sh	1039 sh	1038 sh	1037 vs	1039 s		1041			Coord. anion
1032 m	1031 m	1032 m	1032 m	1032 m	1032 s	1032 m	1032 s	1032 s	1032 s	1032 s	1032 s	1031 s	1032 sh	1030	1032	1032		Free anion
1025 sh	1026 sh	1026 sh	1026 sh	1024 sh	1026 sh	1024 sh	1026 sh	1024 sh	1026 sh	1024 sh	1025 sh	1022 sh	1025 sh	1023	1021			Coord. anion
													769 sh				$\delta_s(CF_3)$	Cryst. complex
													765 sh		763			Coord. anion
	761 sh		761 sh		762 w		762 sh		762 sh		762 sh		761 w					Coord. anion
	756 vw		756 vw		757 w		757 w		757 m		757 m		756 sh					Coord. anion
	752 sh		752 sh		752 sh		753 sh		753 sh		753 sh		753 sh		756	752		Free anion
642 sh		644 sh		643 sh		643 sh		644 sh		646 sh		646 sh					$\delta_s(SO_3)$	Coord. anion
639 m		639 m		638 m		639 s		639 s		639 s		638 vs				637		Free anion
										631 sh		627 sh						Cryst. complex
	583 sh		584 sh		581 sh		582 sh		581 sh		582 sh				583		$\delta_a(CF_3)$	Coord. anion
	573 vw		573 vw		573 w		573 w		573 w		573 w				574	572		Free anion
											570 sh							Cryst. complex
													363 sh				$\rho_r(SO_3)$	Cryst. complex
	352 sh		354 sh		353 sh		355 sh		353 sh		351 sh		353 sh		350			Coord. anion
	347 vw		348 w		347 w		348 m		347 m		347 m		347 w		347	346		Free anion
	321 sh		320 sh		322 sh		321 sh		321 sh		320 sh		321 sh		319		$\nu_s(CS)$	Coord. anion
	313 vw		313 w		314 w		314 m		314 m		313 m		314 m			308		Free anion
													309 sh					Cryst. complex

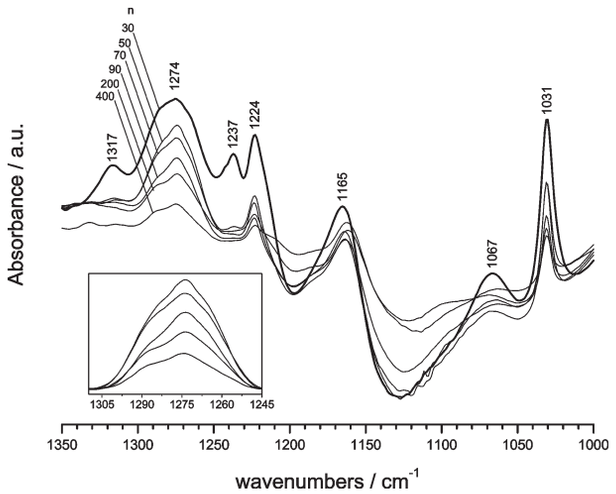

Fig. 3 Subtraction room-temperature FT-IR spectra of the m-Ut(750)$_n$Eu(CF$_3$SO$_3$)$_3$ monourethanesils with $400 \geq n \geq 30$ in the 1350–1000 cm^{-1} region. The inset shows the 1310–1240 cm^{-1} region in more detail.

m-Ut(750)$_{30}$Eu(CF$_3$SO$_3$)$_3$ (Figs. 1 and 3). To gain additional information of the changes undergone by the ν_a(SO$_3$) mode of the monourethanesil xerogels at high Eu(CF$_3$SO$_3$)$_3$ content ($n = 30$ and 10), we performed curve-fitting in the 1345–1200 cm^{-1} frequency envelope. The obtained results lead us to conclude that, apart from the peaks positioned at about 1286, 1274 and 1263 cm^{-1} (already produced by the more dilute samples), four new components exist in the spectra of these two samples near 1317, 1295, 1251 and 1213 cm^{-1}

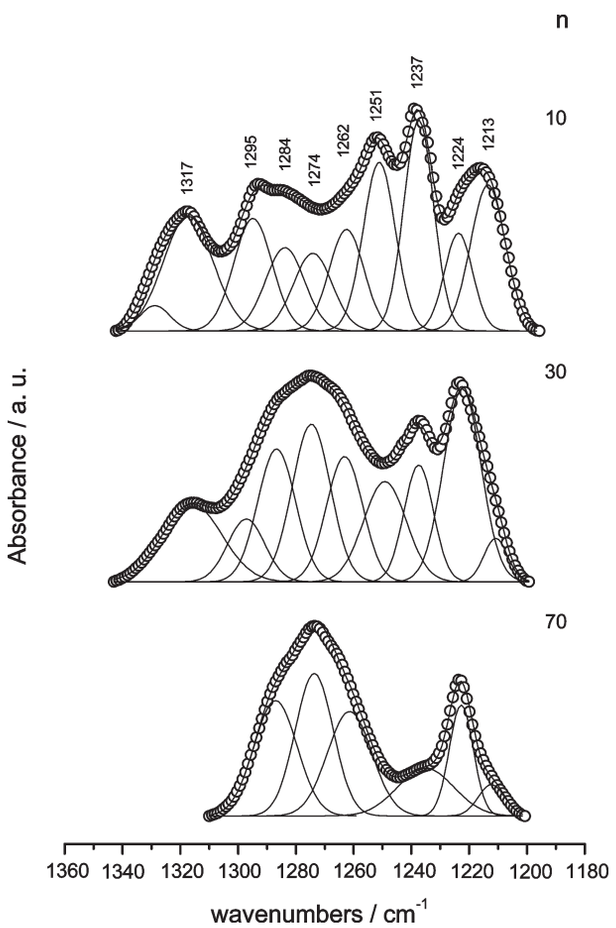

Fig. 4 Curve-fitting results of the subtracted room-temperature FT-IR spectra of selected m-Ut(750)$_n$Eu(CF$_3$SO$_3$)$_3$ monourethanesils in the ν_a(SO$_3$) region.

(Fig. 4, Table 1). These four bands dominate in the ν_a(SO$_3$) envelope of m-Ut(750)$_{10}$Eu(CF$_3$SO$_3$)$_3$ (Fig. 4, Table 1).

ν_s(CF$_3$) and ν_a(CF$_3$) regions. In the FT-IR spectra of the monourethanesils with $n > 30$ the ν_s(CF$_3$) band is found at about 1224 cm^{-1} (Figs. 1 and 3, Table 1). This feature shows intensity growth with salt addition and becomes a prominent band centered at approximately 1237 cm^{-1} in the FT-IR spectra of the two most concentrated samples (Figs. 3 and 4, Table 1). In the case of m-Ut(750)$_{10}$Eu(CF$_3$SO$_3$)$_3$, the 1237 cm^{-1} band is the second strongest absorption feature of the spectrum (Fig. 1).

The ν_a(CF$_3$) band is seen in the FT-IR spectra of the m-Ut(750)-based materials with $n > 10$ as a shoulder situated around 1156 cm^{-1} (Table 1). As already noted in Part 1,[3] the identification of this feature is subject to some uncertainty, because it overlaps the polymer band originated from the coupled vibration of the ν(CO) and ρ_r(CH$_2$) modes, situated near 1142 cm^{-1}. Nevertheless, the IR-difference spectra (Fig. 3) demonstrate that a sharp asymmetric band centered at about 1165 cm^{-1} develops in the spectrum as salt concentration rises. This event becomes a very intense band in the spectrum of the most concentrated sample analyzed (Figs. 1 and 4). It is noteworthy that the broad ν_a(CF$_3$) profile of the latter monourethanesil becomes multicomponent (Fig. 1). It was resolved into five components: a very intense peak situated at about 1170 cm^{-1}, a strong component that appears as a shoulder near 1178 cm^{-1}, and three other less intense shoulders at 1186, 1164 and 1156 cm^{-1} (Table 1).

ν_s(SO$_3$) region. Figs. 1 and 5 (left) evidence that in the ν_s(SO$_3$) region the FT-IR spectra of m-Ut(750)-based compounds with $400 \geq n \geq 30$ exhibit a narrow feature located at 1032 cm^{-1}. Its intensity progressively rises with the incorporation of more Eu(CF$_3$SO$_3$)$_3$, but its position is salt concentration independent. Figs. 2 and 5 (right) show that, in this range of wavenumbers, the Raman spectra of the xerogel materials with $n > 10$ also display a very sharp peak centered at 1032 cm^{-1}, whose intensity grows with salt addition. The ν_s(SO$_3$) envelope was analyzed in more detail by means of 2D correlation spectroscopy. The results of this study will be presented in the next section.

As expected, the spectral signature of the most concentrated material differs deeply from those of the more dilute monourethanesils. Thus in the FT-IR spectrum of this sample two main events at 1037 and 1032 cm^{-1} and two shoulders situated at 1042 and 1022 cm^{-1} are evident (Fig. 5 (left), Table 1). The corresponding Raman spectrum exhibits a strong band at 1039 cm^{-1} and shoulders at 1045, 1032 and 1025 cm^{-1} (Figs. 5 (right) and 6, Table 1).

δ_s(CF$_3$) region. In the FT-IR spectra of the doped monourethanesils the δ_s(CF$_3$) mode appears as a very weak to weak, ill-defined event (Fig. 1). Fig. 7 (left) shows that the intensity maximum of this band is progressively shifted toward higher wavenumbers as more salt is incorporated into the m-Ut(750) matrix (about 754, 756 and 765 cm^{-1} in the FT-IR spectra of the compounds with $n = 400$, 30 and 10, respectively).

The FT-Raman spectra illustrated in Fig. 2 allow us to conclude that in the δ_s(CF$_3$) region the Eu^{3+}-doped monourethanesils with $400 \geq n \geq 30$ produce a sharp, weak to medium intensity feature, whose intensity maximum is displaced from approximately 755 cm^{-1} in the most dilute material to 757 cm^{-1} in the sample with $n = 30$. In the spectrum of the most concentrated sample this band becomes significantly broader and weaker and its intensity maximum appears at 761 cm^{-1} (Fig. 2). In addition, a shoulder located around 769 cm^{-1} emerges (Fig. 7 (right)). A closer consideration of this spectral

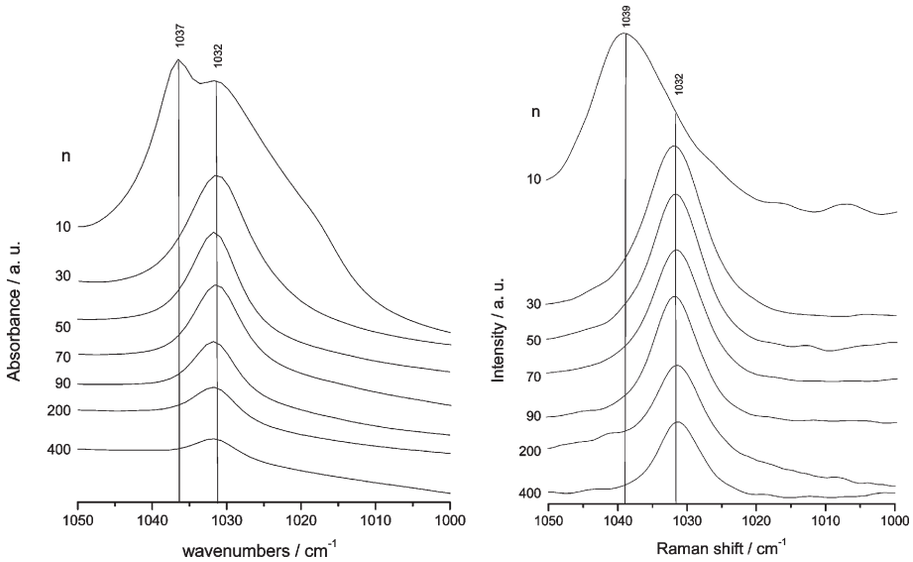

Fig. 5 Room-temperature FT-IR (left) and FT-Raman (right) spectra of the m-Ut(750)$_n$Eu(CF$_3$SO$_3$)$_3$ monourethanesils in the ν_s(SO$_3$) region. In order to examine exclusively the contribution of the ν_s(SO$_3$) mode, the FT-Raman spectrum of the pure polymer had to be first subtracted from those of the hybrids with $400 \geq n \geq 30$.

range clearly suggests, however, that several components can be resolved in this region. A deeper investigation of the δ_s(CF$_3$) eature will be performed in the following section.

700–300 cm^{-1} region. Between 700 and 500 cm^{-1} the spectrum of the "free" triflate ion displays a band of the symmetric deformation vibration of the SO$_3$ group, δ_s(SO$_3$), around 637 cm^{-1} and a peak, originated from the asymmetric deformation vibration of the CF$_3$ group, δ_a(CF$_3$), positioned at about 572 cm^{-1}.[9] On coordination of the anion to metal cations, both features shift to higher wavenumbers.[9,14*b*,19*b*] In the 500–300 cm^{-1} envelope, a non-bonded CF$_3$SO$_3^-$ ion produces two spectral bands around 346 and 308 cm^{-1} ascribed to the rocking vibration of the SO$_3$ group, ρ_r(SO$_3$), and to the symmetric stretching vibration of the CS group, ν_s(CS), respectively.[9] These two modes are also upshifted upon coordination.[9,14*b*,19*b*]

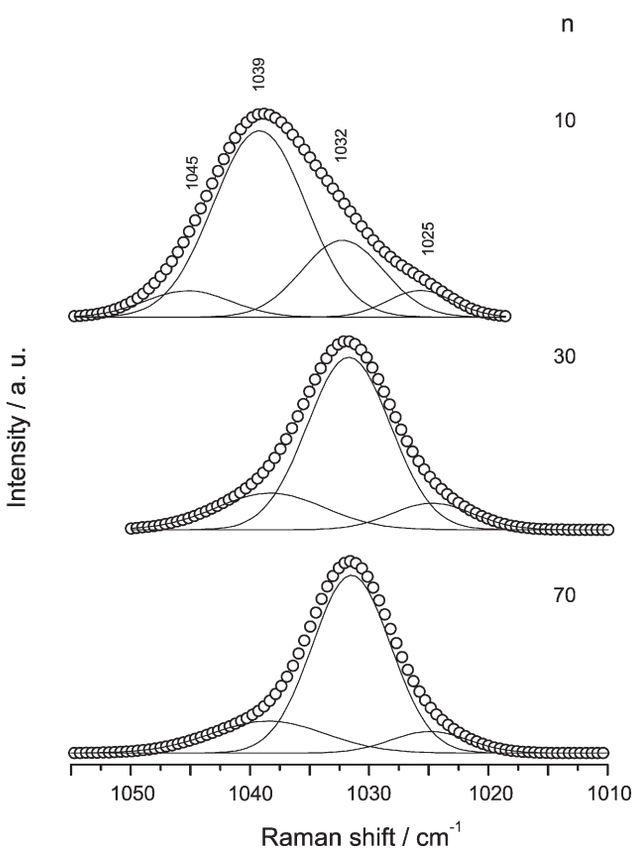

Fig. 6 Curve-fitting results of the room-temperature FT-Raman spectra of selected m-Ut(750)$_n$Eu(CF$_3$SO$_3$)$_3$ monourethanesils in the ν_s(SO$_3$) region. In order to examine exclusively the contribution of the ν_s(SO$_3$) mode, the FT-Raman spectrum of the pure polymer had to be first subtracted from those of the hybrids with $400 \geq n \geq 30$.

In the FT-IR spectra of the monourethanesil compounds under investigation the δ_s(SO$_3$) band is a sharp feature found at 639 cm^{-1}, whose intensity progressively increases with the addition of lanthanide salt (Fig. 1, Table 1). In the FT-IR spectrum of m-Ut(750)$_{10}$Eu(CF$_3$SO$_3$)$_3$ sample this mode becomes a very strong event (Fig. 1, Table 1). A shoulder located near 644 cm^{-1} is also detected in the FT-IR spectra of the monourethane xerogels in the whole range of salt concentration (Table 1).

A comprehensive curve-fitting allowed us to conclude that the m-Ut(750)$_n$Eu(CF$_3$SO$_3$)$_3$ hybrids with $400 \geq n \geq 30$ produce in the FT-Raman spectra a very weak to weak band at about 573 cm^{-1} with a shoulder situated around 582 cm^{-1} (Table 1). The characteristic ρ_r(SO$_3$) and ν_s(CS) bands are discerned in the same spectra near 347 and 314 cm^{-1}, respectively (Fig. 2, Table 1). Their intensity is enhanced with the incorporation of increasing amounts of the guest salt. In addition, two shoulders are found at 353 and 321 cm^{-1} (Table 1). At $n = 30$, two other shoulders located at approximately 631 and 570 cm^{-1} appear in the FT-IR and FT-Raman spectra, respectively (Table 1). Upon further addition of the guest salt (m-Ut(750)$_{10}$Eu(CF$_3$SO$_3$)$_3$) the former shoulder shifts to 627 cm^{-1} and the latter one vanishes. In addition two new shoulders situated at 363 and 309 cm^{-1} emerge in the FT-Raman spectrum (Table 1).

2 Two-dimensional spectroscopic correlation analysis

In order to investigate in depth the changes of the spectral intensities occurring in δ_s(CF$_3$) and ν_s(SO$_3$) frequency envelopes as a function of salt concentration, we performed a 2D Correlation FT-IR and Raman spectroscopic study on the set of materials with $400 \geq n \geq 30$. The sample with $n = 10$ was excluded from this analysis because its vibrational

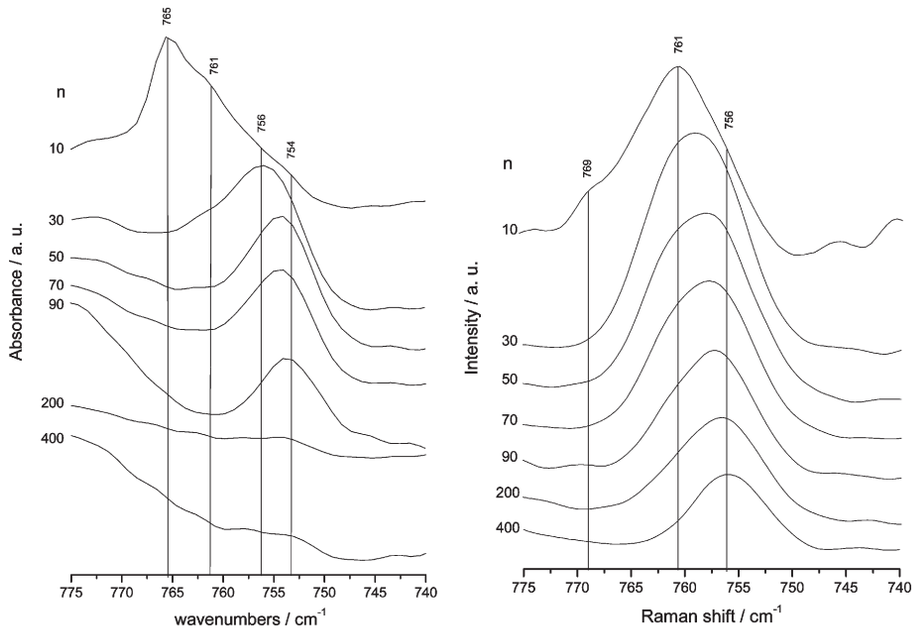

Fig. 7 Room-temperature FT-IR (left) and FT-Raman (right) spectra of the m-Ut(750)$_n$Eu(CF_3SO_3)$_3$ monourethanesils in the $\delta_s(CF_3)$ region.

spectrum exhibits crucial transformations originating from drastic reconfiguration of the polymer matrix.[3]

The main goal of 2D correlation vibrational spectroscopy is to detect dynamic variations of spectroscopic signals induced by an external perturbation, which in the present case was the incorporation of different amounts of $Eu(CF_3SO_3)_3$. In dynamic vibrational spectra, typical changes are variations of band intensity, frequency shifts of the bands and modifications in the shape of the peaks. The detected spectral change is then transformed in 2D spectra by means of a specialized correlation method, such as the one described in the Experimental section. As a result of this transformation, one obtains two 2D correlation spectra generally called synchronous and asynchronous maps. Correlation peaks appearing in the synchronous and asynchronous maps represent in-phase and out-of-phase variation tendencies of corresponding band intensities, respectively. It should be also stressed that 2D correlation analysis is a powerful tool for the determination of the number of spectral components in strongly overlapped profiles.[22]

To elucidate the question about the local coordination of the $CF_3SO_3^-$ ions, it was important to examine the spectral region characteristic of the $\delta_s(CF_3)$ mode, which has been found to be extremely sensitive to the environmental changes around the anion.[10*a–d*,10*f–r*] The synchronous 2D correlation Raman spectra obtained for the series of monourethane cross-linked xerogels with $200 \geq n \geq 30$ in the 770–750 cm^{-1} frequency region (Fig. 8 (top)) displays a single peak located on the diagonal of 2D correlation map with the coordinate of 761 cm^{-1}. We must note that the peaks at diagonal positions, designated as *autopeaks*, develop in the spectral intervals which demonstrate stronger intensity change with the external perturbation.[22] Consequently, the 2D correlation analysis indicates that, as salt content rises, the strongest intensity change appears around 761 cm^{-1}, *i.e.*, at a characteristic frequency of coordinated triflate species. This means that, as more $Eu(CF_3SO_3)_3$ is introduced into the m-Ut(750) matrix, the concentration of the triflate environment responsible for the 761 cm^{-1} component increases in the xerogels. The growth of this event is clearly evidenced in the Raman spectra of the m-Ut(750)$_n$Eu(CF_3SO_3)$_3$ compounds with $200 \geq n \geq 30$ (Fig. 7 (right)).

The asynchronous 2D correlation map derived for the same set of monourethanesil samples in the same range of frequencies is given in Fig. 8 (bottom). It is believed that cross peaks (*i.e.*, off-diagonal peaks) in asynchronous 2D spectra usually

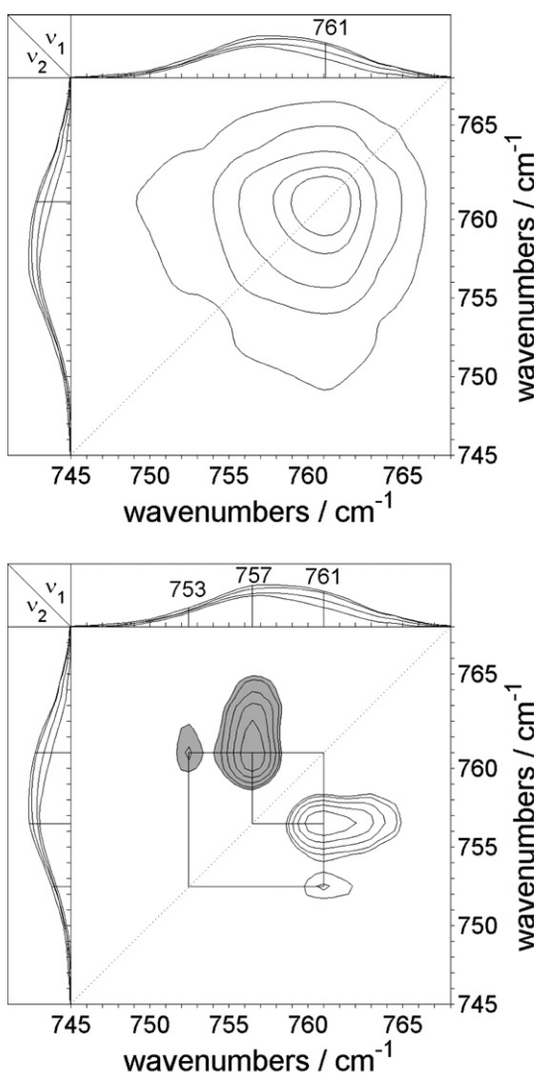

Fig. 8 Synchronous (top) and asynchronous (bottom) 2D-FT-Raman contour maps calculated for the m-Ut(750)$_n$Eu(CF_3SO_3)$_3$ monourethanesils with $200 \geq n \geq 30$ in the $\delta_s(CF_3)$ region. Positive cross-peaks are white, whereas negative cross-peaks are grey.

indicate the lack of strong chemical interactions or direct connectivity between the functional groups. They appear rather due to a difference in reorientational rates of transition moments of the functional groups which are located in different local molecular environments.[22] By extending lines from the spectral coordinates of the cross peaks to the corresponding diagonal positions, one obtains the frequencies at which the maximum variation of spectral intensities is observed.[22] Thus the map shown in Fig. 8 (bottom) suggests that there are three distinct components located at 761, 757 and 753 cm^{-1} in the $\delta_s(CF_3)$ band envelope. Based on these results we carried out curve-fitting of the $\delta_s(CF_3)$ envelope. The $\delta_s(CF_3)$ region of the monourethanesils with $400 \geq n \geq 30$ was decomposed into three components centered at about 762, 757 and 753 cm^{-1} (Fig. 9, Table 1). The band at lowest frequency is associated with "free" anions,[9] whereas the other two are due to coordinated $CF_3SO_3^-$ ions. In the spectrum of the sample with $n = 10$ two additional peaks are seen at 769 and 765 cm^{-1} (Fig. 9, Table 1). The latter event is assigned to coordinated anions. The 769 cm^{-1} feature must be characteristic of the crystalline compound.[3]

Fig. 10 shows the contour of the asynchronous 2D correlation map constructed from the salt concentration perturbed FT-IR spectra of the monourethanesils with $200 \geq n \geq 30$ in the 1045–1020 cm^{-1} region. This map exhibits four cross peaks, two of positive and two of negative intensity. Hence, in the investigated $\nu_s(SO_3)$ envelope three spectral components centered at 1036, 1032 and 1026 cm^{-1} may be resolved (Fig. 10). Similar conclusions were obtained through curve-fitting (Fig. 6, Table 1). The most intense peak, located at 1032 cm^{-1}, is attributed to the 'free' triflate anions.[9] The pair of events at 1036 and 1026 cm^{-1} may be associated with coordinated anions in two different ionic environments.[19b,20a]

It must be noted at this stage that the band observed in the 1045–1020 cm^{-1} spectral interval may be fitted with a good accuracy by a single Lorentzian peak (especially at low salt contents). In two Raman studies of ion association in complexes formed between POE or poly(oxypropylene) and triflate salts containing mono-, di- and trivalent cations, it was shown that the 1032 cm^{-1} band, characteristic of the "free" triflate ion, always demonstrated Lorentzian shape regardless the type

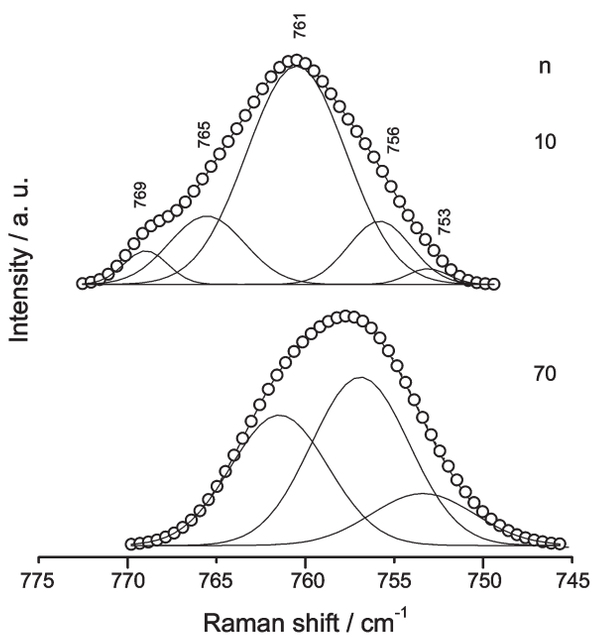

Fig. 9 Curve-fitting results of the room-temperature FT-Raman spectra of selected m-Ut(750)$_n$Eu$(CF_3SO_3)_3$ monourethanesils in the $\delta_s(CF_3)$ region.

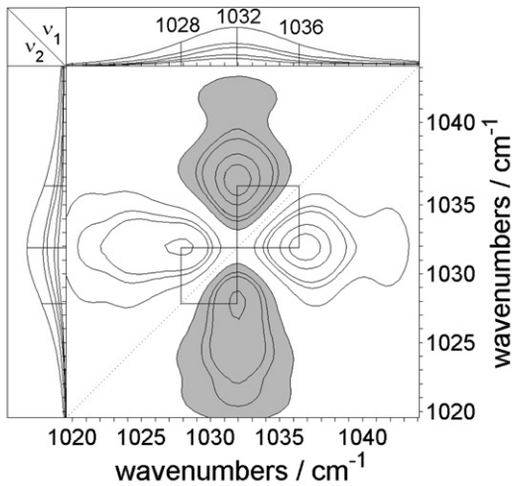

Fig. 10 Asynchronous 2D-FT-IR contour map calculated for the m-Ut(750)$_n$Eu$(CF_3SO_3)_3$ monourethanesils with $200 \geq n \geq 30$ in the $\nu_s(SO_3)$ region. Positive cross-peaks are white, whereas negative cross-peaks are grey.

of cation.[18a,b] However, it is essential to remark that, while in the Raman spectra reported in refs. 18*a* and *b* the half-width of the 1032 cm^{-1} feature was about 5.5 cm^{-1} (with the highest value of 7 cm^{-1} detected in a material doped with Nd^{3+} ions), in the spectra of the xerogels investigated in the present work the fit by a single Lorentzian curve produces a peak with half-width of 9.5 cm^{-1} for the low concentration samples, which further increases up to 11.5 cm^{-1} as the guest salt content rises. Under such conditions it is clear that fitting by a single Lorentzian shape may hide the presence of side bands of lower intensity. Therefore, in the selection of the fitting parameters we took into account the three following factors: (i) the unexplainably large half-width found when the band was fitted by a single Lorentzian profile; (ii) the high probability of existence of differently coordinated triflate species; (iii) the results derived from the 2D correlation analysis performed in this frequency envelope (Fig. 10). Since we do not use the curve-fitting data for the determination of the total integral intensities, but just to estimate frequency positions of the components, we believe that the present analysis is reliable.

3 Triflate ion bonding configurations

In this section we will attempt to deduce, on the basis of specific spectral triflate features, the bonding configurations of the anions in the m-Ut(750)$_{10}$Eu$(CF_3SO_3)_3$ family of xerogels to gain more insight into the general picture of ionic association in these hybrids.

In the $400 \geq n \geq 50$ composition range, the characteristic $\nu_a(SO_3)$ envelope contains three bands located at about 1286, 1275 and 1263 cm^{-1} (Figs. 3 and 4). The 1275 cm^{-1} band is attributed to "free" $CF_3SO_3^-$ ions,[8,9] whereas the origin of the two other components is not straightforward. It is known that a strong interaction between the SO_3 group and the cation, such as that involved in a contact ion pair, lifts the double degeneracy of the $\nu_a(SO_3)$ mode, thus leading to the appearance of two split bands. According to the observations of Bernson *et al.*,[20a,b] the typical $\nu_a(SO_3)$ splitting values for contact ion pairs in polymer electrolytes containing lanthanide triflates range from 95 to 110 cm^{-1}, depending on the type of polymer matrix, type of cation used, and salt concentration. In the case of solvent-separated ion pairs, in which the strength of cation–anion interaction becomes essentially lower, the magnitude of the splitting was found to be *ca.* 40 cm^{-1}.[20b] In the monourethanesils with $400 \geq n \geq 50$ the splittings observed

are significantly smaller (about 25 cm^{-1}), thus suggesting that the species responsible for this effect can be neither contact ion pairs, nor solvent separated ion pairs. The fact that the three-component profile is also detected in the spectra of the monourethanesils with extremely low salt content ($n = 400$ and 200), in which the formation of contact ion pairs is practically impossible, is consistent with our claim. We propose that the remarkably small $\nu_a(SO_3)$ splitting produced by the m-Ut(750)$_n$Eu$(CF_3SO_3)_3$ samples with $400 \geq n \geq 50$ is a direct consequence of the weakness of the interaction existent between the $CF_3SO_3^-$ and the Eu^{3+} ions. We may further speculate that this coordinating situation could involve $CF_3SO_3^-$ species weakly bonded to Eu^{3+} ions, which simultaneously interact with the carbonyl oxygen atoms of the urethane groups (A). In addition, the existence of $CF_3SO_3^-$ ions hydrogen-bonded to the N–H groups cannot be excluded (B).

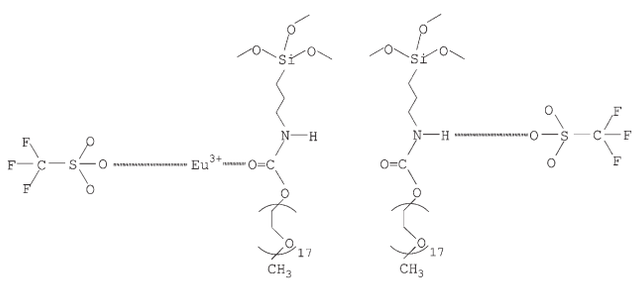

A B

When the salt content reaches $n = 30$, the behavior of the monourethanesil system suffers marked modifications. As was shown in Part 1,[3] at this particular composition new effects are produced: (1) a fraction of the N–H groups start to be free from hydrogen bonding interaction with the C=O groups; (2) the lanthanide ions start to coordinate to the POE chains. Fig. 4 shows that in the $\nu_a(SO_3)$ region of the FT-IR spectrum of m-Ut(750)$_{30}$Eu$(CF_3SO_3)_3$, along with the 1284/1262 cm^{-1} pair and the 1274 cm^{-1} feature, new split components, which can be recognized as the 1295/1251 and 1317/1213 cm^{-1} pairs, emerge (Table 1).

Bands at 1295 and 1251 cm^{-1} were also detected in the spectra of poly(ethylene glycol)/La$(CF_3SO_3)_3$ electrolytes.[20b] These events were ascribed to the split components resulting from the presence of solvent separated ion pairs. In the monourethane cross-linked hybrids such spectral effect might appear due to the presence of "cross-link separated" ion pairs. The POE chains probably contribute to the formation of the latter ionic aggregates.

The 1317/1213 cm^{-1} pair observed in the FT-IR spectrum of the xerogel with $n = 30$ can be associated with contact ion pairs, since similar bands were seen at approximately the same position in the spectra of POE$_n$Eu$(CF_3SO_3)_3$ electrolytes with $n = 16$ and 9.[20a]

At the highest salt concentration examined here ($n = 10$), the growth of the bands corresponding to the second and third coordinating environments just described and the reduction of those due to the "free" and weakly coordinated triflate ions are evident.

In the $\nu_s(CF_3)$ region of all the monourethanesils studied the appearance of the 1224 and 1237 cm^{-1} features corroborates the claim that "free"[9] and coordinated triflate ions[9,20a,b] exist within the whole range of salt concentrations investigated (Figs. 1 and 4, Table 1).

The existence of non-coordinated anions in the materials with $400 \geq n \geq 30$ is also supported by the location of the $\nu_a(CF_3)$ mode which is seen at approximately 1156 cm^{-1}.[8] The bands found at 1186, 1178, 1170, 1164 and 1156 cm^{-1} in the $\nu_a(CF_3)$ envelope of the FT-IR spectrum of m-Ut(750)$_{10}$Eu$(CF_3SO_3)_3$ (Table 1) confirm that non-bonded anions subsist at this composition and strongly suggest that the anion is involved in four different coordinating environments in this salt-rich xerogel, a result that is in perfect agreement with the conclusions retrieved from the $\nu_a(SO_3)$ region.

The presence of "free" anions in the doped monourethanesils (a conclusion drawn from the examination of the $\nu_a(SO_3)$, $\nu_s(CF_3)$ and $\nu_a(CF_3)$ regions) is further confirmed by the appearance of the 1032 cm^{-1} band, characteristic of the $\nu_s(SO_3)$ vibration of the "free" triflate ion (Figs. 1, 2 and 6, Table 1). The occurrence of two components on both sides of the 1032 cm^{-1} feature in the spectra of the hybrids with $n > 10$ (Fig. 6, Table 1) corroborates the results of the $\nu_a(SO_3)$ region, which indicated that two anionic bonding environments exist in this salt concentration interval (Figs. 1, 3 and 4, Table 1)

It must be stressed that in the sample with $n = 10$ the number of $\nu_s(SO_3)$ components that represent distinct anionic sites (*i.e.*, three) is in apparent contradiction with the information obtained from the analysis of the $\nu_a(SO_3)$ band envelope which indicated the existence of four different anionic configurations. This effect can, however, be explained on the basis of the conclusions of Petersen *et al.*[18b] who showed that the $\nu_s(SO_3)$ mode of solvent separated ions appears at 1032 cm^{-1}, typically ascribed to "free" $CF_3SO_3^-$ ions. Therefore, we are led to suggest that the 1032 cm^{-1} component discerned in the spectrum of the rich-salt hybrid with $n = 10$ most probably receives contributions from, not only the "free" anions, as usual, but also from the "cross-link separated" ion pairs.

As it is beyond the scope of the present work to characterize the ionic aggregates responsible for the multicomponent $\nu_s(SO_3)$ band profile of the m-Ut(750)-based compounds, we will simply consider that the two shoulders observed in the $\nu_s(SO_3)$ region of the samples with $400 \geq n \geq 30$ are originated from weakly coordinated $CF_3SO_3^-$ ions (Table 1). The 1042 cm^{-1} (FT-IR)/1045 cm^{-1} (Raman) component of m-Ut(750)$_{10}$Eu$(CF_3SO_3)_3$ is tentatively attributed to the formation of the crystalline compound (Fig. 6, Table 1).

Considering the complicated behavior of the $\nu_s(SO_3)$ vibration, it was proposed that the mode of symmetric CF_3 deformation, $\delta_s(CF_3)$, is a much more reliable way of identifying differently coordinated $CF_3SO_3^-$ ions.[10a–d,f–r] According to Frech *et al.*,[10a–d,f–r] although the CF_3 end of the anion is not expected to participate directly in the coordination process, cation–anion interactions affect the whole anion. The $\delta_s(CF_3)$ vibration is seen at about 752 cm^{-1} when the ion is "free".[9] As this mode is non-degenerate, specific bonding geometries result in shifts to higher wavenumbers.

The interpretation of the $\delta_s(CF_3)$ envelope of the Eu^{3+}-doped monourethanesils is not straightforward. The only reference found in the literature regarding the $\delta_s(CF_3)$ region of lanthanide triflate electrolytes[20b] reports the presence of a dominating band centered at 762 cm^{-1} and a less intense peak at 754 cm^{-1} in the spectra of La$(CF_3SO_3)_3$ dissolved in poly(ethylene glycol) methyl ether. The two events were assigned to ion pairs and "free" anions, respectively.[20b] In the present case, the complexity of the band contour clearly suggests that the number of underlying components is much greater. The examination of the $\delta_s(CF_3)$ region of the most concentrated monourethanesil allowed us to conclude about the existence of four coordinating sites. In the case of the less concentrated xerogels, the 2D correlation analysis clearly showed the presence of two coordinating environments. This finding means that, according to our spectral data, in samples with $n = 10$ and $n > 10$ the anionic configurations deduced from the study of the $\delta_s(CF_3)$ mode (*i.e.*, four and two, respectively) are identical to those derived from the other triflate regions analyzed above.

In the low-frequency region of the spectra of the m-Ut(750)$_n$Eu$(CF_3SO_3)_3$ composites, unmistakable evidences of the existence of unpaired and coordinated $CF_3SO_3^-$ ions are apparent in the whole range of salt concentration (Table 1).

The new shoulders detected in the spectra of the samples with $n = 30$ and 10 are tentatively associated with the crystalline complex formed at this composition (Table 1).

It is finally instructive to mention that in the course of this investigation we recorded the FT-IR spectra of the monourethanesils in the temperature range between 20 and 85 °C (data not shown). The spectra of all the samples were found to be temperature independent, an indication that the existing cation and anion coordinating environments are quite stable.

Conclusions

Monourethane cross-linked poly(oxyethylene)/siloxane hybrids incorporating a wide range of europium triflate, $Eu(CF_3SO_3)_3$, concentration ($\infty \geq n \geq 10$, where n is the molar ratio of (OCH_2CH_2) repeat units per Eu^{3+} ion) were investigated by means of Fourier transform mid-IR and Raman spectroscopies to study the cation–anion interactions.

This spectroscopic analysis relied essentially on the examination of the most informative bands of the triflate ion (in particular, the $\nu_a(SO_3)$, $\nu_s(SO_3)$ and $\delta_s(CF_3)$ modes) at increasing salt concentration. Two-dimensional correlation spectroscopic analysis was employed in the case of the $\nu_s(SO_3)$ and $\delta_s(CF_3)$ features that exhibited strong overlapped profiles.

This work showed that in the m-Ut(750)$_n$Eu$(CF_3SO_3)_3$ xerogels with $400 \geq n \geq 50$ the triflate ions exist only as "free" and weakly coordinated species (O(triflate)$\cdots$$Eu^{3+}$$\cdots$O=C(urethane) and/or O(triflate)$\cdots$H–N(urethane)). At $n = 30$, in addition to these coordinating situations, two new ionic configurations appear: contact ion pairs and "cross-link separated" ion pairs. These two environments are a consequence of the major modification undergone by the system involving the reconfiguration of the POE chains and the destruction of the hydrogen bonds established between N–H groups and carbonyl moieties or POE chains. In the most concentrated sample analyzed ($n = 10$) direct cation–anion coordination becomes dominating and the formation of a crystalline polymer/salt complex is observed.

Experimental

Synthesis

See Part 1.[3]

Fourier transform IR spectroscopy

See Part 1.[3]

Fourier transform Raman spectroscopy

See Part 1.[3]

Two dimensional (2D) correlation spectroscopic analysis

In 2D spectroscopy, the variations in the spectra produced by an external sample perturbation are mathematically cross-correlated to construct a 2D correlation map, which allows to discriminate those vibration modes which selectively respond to the perturbation. Two kinds of 2D spectra, defined by two independent wavenumbers (ν_1, ν_2), are generated by cross-correlation analysis of dynamic fluctuations of spectral signals induced by an external perturbation: the synchronous and asynchronous spectra.[22] While the synchronous 2D correlation spectrum represents the simultaneous (or coincidental) changes of spectral intensities measured at ν_1 and ν_2 within the interval between T_{min} and T_{max} of the externally defined variable t, the asynchronous one represents sequential (or successive) changes of spectral intensities measured at ν_1 and ν_2.

In the present work 2D correlation spectroscopic analysis was carried out using the following procedure. First, the reference spectrum was subtracted from each of the experimental spectra in order to obtain the dynamic spectra (mean-centered procedure[22]). For practical reasons, in our calculations the average spectrum was used as a reference. The resulting mean-centered dynamic spectra $y(\nu,t)$ represent the relative variations of spectral intensity at each wavenumber ν as a function of the lanthanide salt concentration t. We then calculated, for the set of dynamic spectra, the complex correlation function $\langle y(\nu_1,t), y(\nu_2,t')\rangle = \Phi(\nu_1,\nu_2) + i\Psi(\nu_1,\nu_2)$ using the Hilbert transform algorithm developed by Noda.[22] The real and imaginary parts of this function correspond to the synchronous $\Phi(\nu_1,\nu_2)$ and asynchronous $\Psi(\nu_1,\nu_2)$ 2D correlation maps of the dynamic spectra, respectively. The synchronous 2D correlation intensities were defined by the equation

$$\Phi(\nu_1,\nu_2) = \frac{1}{n-1}\sum_{j=1}^{n} y(\nu_1,t_j)\,y(\nu_2,t_j), \qquad (1)$$

and the asynchronous 2D spectra were determined using the expression

$$\Psi(\nu_1,\nu_2) = \frac{1}{n-1}\sum_{j=1}^{n} y(\nu_1,t_j)\sum_{k=1}^{n} H_{jk}\,y(\nu_2,t_k) \qquad (2)$$

where the H_{jk} is a Hilbert transformation matrix.[22]

$$H_{jk} = \begin{cases} 0 & \text{if } j = k \\ 1/\pi(k-j) & \text{otherwise} \end{cases} \qquad (3)$$

Here ν represents the IR or Raman wavenumber and n is the total number of dynamic spectra. All the calculations were performed with the Matlab 6.0 software (The MathWorks Inc.).

Acknowledgements

This work was supported by Fundação para a Ciência e Tecnologia (contracts POCTI/P/CTM/33653/00 and POCTI/CTM/46780/02). D. O. and S. L. acknowledge financial support from Veteskapsrådet (Sweden) program and Svenska Institute, respectively. M. C. G. thanks Fundação Calouste Gulbenkian for a grant.

References

1 V. de Zea Bermudez, M. C. Gonçalves and L. D. Carlos, *Ionics*, 1999, **5**(3&4), 251–260.
2 V. de Zea Bermudez, L. Alcácer, J. L. Acosta and E. Morales, *Solid State Ionics*, 1999, **116**, 197–209.
3 V. de Zea Bermudez, D. Ostrovskii, M. C. Gonçalves, L. D. Carlos, R. A. Sá Ferreira, L. Reis and P. Jacobsson, *Phys. Chem. Chem. Phys.*, 2004, **6**, 10.1039/b308201f.
4 (*a*) M. Armand, C. Poinsignon, J.-Y. Sanchez and V. de Zea Bermudez, *US. Pat.*, 5,283,310, 1994; (*b*) V. de Zea Bermudez, C. Poinsignon and M. Armand, *J. Mater. Chem.*, 1997, **7**(9), 1677–1692.
5 (*a*) K. Dahmouche, M. Atik, N. C. Mello, T. J. Bonagamba, H. Panepucci and M. A. Aegerter, *J. Sol–Gel Sci. Technol.*, 1997, **8**, 711–715; (*b*) S. J. L. Ribeiro, K. Dahmouche, C. A. Ribeiro, C. V. Santilli and S. H. Pulcinelli, *J. Sol–Gel Sci. Technol.*, 1998, **13**, 427–432.
6 (*a*) V. Bekiari, P. Lianos and P. Judeinstein, *Chem. Phys. Lett.*, 1999, **307**, 310–316; (*b*) V. Bekiari, P. Lianos, U. L. Stangar, B. Orel and P. Judeinstein, *Chem. Mater.*, 2000, **12**, 3095–3099.
7 (*a*) L. D. Carlos, V. de Zea Bermudez, M. C. Duarte, M. M. Silva, C. J. Silva, M. J. Smith, M. Assunção and L. Alcácer, in *Physics and Chemistry of Luminescent Materials VI*, ed. C. Ronda and T. Welker, Electrochemical Society Proceedings, San Francisco, CA, 1997, vol. 97–29, pp. 352–367; (*b*) V. de Zea Bermudez, L. D. Carlos, M. C. Duarte, M. M. Silva, C. J. Silva, M. J. Smith, M. Assunção and L. Alcácer, *J. Alloys Compd.*, 1998, **275–277**,

21–26; (*c*) L. D. Carlos, V. de Zea Bermudez and R. A. Sá Ferreira, *J. Non-Cryst. Solids*, 1999, **247**, 203–208; (*d*) M. M. Silva, V. de Zea Bermudez, L. D. Carlos, A. P. Passos de Almeida and M. J. Smith, *J. Mater. Chem.*, 1999, **9**, 1735–1740; (*e*) V. Zea Bermudez, L. D. Carlos and L. Alcácer, *Chem. Mater.*, 1999, **11**(3), 569–580; (*f*) L. D. Carlos, R. A. Sá Ferreira, V. de Zea Bermudez, C. Molina, L. A. Bueno and S. J. L. Ribeiro, *Phys. Rev. B*, 1999, **60**(14), 10 042–10 053; (*g*) M. M. Silva, V. de Zea Bermudez, L. D. Carlos and M. J. Smith, *Electrochim. Acta*, 2000, **45**, 1467–1471; (*h*) L. D. Carlos, Y. Messaddeq, H. F. Brito, R. A. Sá Ferreira, V. de Zea Bermudez and S. J. L. Ribeiro, *Adv. Mater.*, 2000, **12**(8), 594–598; (*i*) L. D. Carlos, R. A. Sá Ferreira, I. Orion, V. de Zea Bermudez and J. Rocha, *J. Lumin.*, 2000, **87–89**, 702–705; (*j*) L. D. Carlos, R. A. Sá Ferreira, V. de Zea Bermudez and S. J. L. Ribeiro, *Adv. Funct. Mater.*, 2001, **11**(2), 111–115; (*k*) V. de Zea Bermudez, R. A. Sá Ferreira, L. D. Carlos, C. Molina, K. Dahmouche and S. J. L. Ribeiro, *J. Phys. Chem.*, 2001, **105**(17), 3378–3386; (*l*) V. Amaral, L. D. Carlos and V. de Zea Bermudez, *IEEE Trans. Magn.*, 2001, **37**(4), 2935–2937.

8 (*a*) Å. Wendsjö, J. Lindgren and C. Paluszkiewicz, *Electrochim. Acta*, 1992, **37**(9), 1689–1693; (*b*) Å. Wendsjö, J. Lindgren, J. O. Thomas and G. C. Farrington, *Solid State Ionics*, 1992, **53–56**, 1077–1082.

9 D. H. Johnston and D. F. Shriver, *Inorg. Chem.*, 1993, **32**, 1045–1047.

10 (*a*) J. Manning and R. Frech, *Polymer*, 1992, **33**(16), 3487–3494; (*b*) W. Huang, R. Frech and R. A. Wheeler, *J. Phys. Chem.*, 1994, **98**, 100–110; (*c*) W. Huang and R. Frech, *Polymer*, 1994, **35**(2), 235–242; (*d*) W. Huang, R. Frech, P. Johansson and J. Lindgren, *Electrochim. Acta*, 1995, **40**(13–14), 2147–2151; (*e*) P.-Å. Bergström and R. Frech, *J. Phys. Chem.*, 1995, **99**, 12 603–12 611; (*f*) M. A. K. L. Dissanayake and R. Frech, *Macromolecules*, 1995, **28**(15), 5312–5319; (*g*) R. Frech and S. Chintapalli, *Solid State Ionics*, 1996, **85**, 61–66; (*h*) S. Chintapalli, C. Zea and R. Frech, *Solid State Ionics*, 1996, **92**, 205–212; (*i*) S. Chintapalli and R. Frech, *Macromolecules*, 1996, **29**, 3499–3506; (*j*) S. Chintapalli, C. Quinton, R. Frech and C. A. Vincent, *Macromolecules*, 1997, **30**, 7472–7477; (*k*) R. Frech, S. Chintapalli, P. Bruce and C. A. Vincent, *Chem. Commun.*, 1997, 157–158; (*l*) S. Chintapalli and R. Frech, *Electrochim. Acta*, 1998, **43**(10–11), 1395–1400; (*m*) C. P. Rhodes and R. Frech, *Solid State Ionics*, 1999, **121**, 91–99; (*n*) C. P. Rhodes, B. Kiassen, R. Frech, Y. Dai and S. G. Greenbaum, *Solid State Ionics*, 1999, **126**, 251–257; (*o*) R. Frech, S. Chintapalli, P. G. Bruce and C. A. Vincent, *Macromolecules*, 1999, **32**, 808–813; (*p*) C. P. Rhodes and R. Frech, *Solid State Ionics*, 2000, **136–137**, 1131–1137; (*q*) S. York, R. Frech, A. Snow and D. Glatzhofer, *Electrochim. Acta*, 2001, **46**, 1533–1537; (*r*) S. York, E. C. Kellam III, H. R. Allcock and R. Frech, *Electrochim. Acta*, 2001, **46**, 1553–1557.

11 (*a*) B. L. Papke, M. A. Ratner and D. F. Shriver, *J. Phys. Chem. Solids*, 1981, **42**, 493–500; (*b*) B. L. Papke, M. A. Ratner and D. F. Shriver, *J. Electrochem. Soc.*, 1982, **129**(7), 1434–1438.

12 (*a*) D. R. MacFarlane, P. Meakin, A. Bishop, D. McNaughton, J. M. Rosalie and M. Forsyth, *Electrochim. Acta*, 1995, **40**(13–14), 2333–2337; (*b*) A. Bishop, D. R. MacFarlane, D. McNaughton and M. Forsyth, *J. Phys. Chem.*, 1996, **100**, 2237–2243; (*c*) A. Bishop, D. R. MacFarlane and D. McNaughton, *Solid State Ionics*, 1996, **85**, 129–135; (*d*) M. Forsyth, J. Sun and D. R. MacFarlane, *Solid State Ionics*, 1998, **112**, 161–163.

13 (*a*) A. Ferry, P. Jacobsson and L. M. Torell, *Electrochim. Acta*, 1995, **40**(13–14), 2369–2373; (*b*) A. Ferry, P. Jacobsson and J. R. Stevens, *J. Phys. Chem.*, 1996, **100**, 12 574–12 582; (*c*) A. Ferry, G. Orädd and P. Jacobsson, *Macromolecules*, 1997, **30**, 7329–7331; (*d*) A. Ferry and M. Tian, *Macromolecules*, 1997, **30**, 1214–1215; (*e*) A. Ferry, *J. Chem. Phys.*, 1997, **107**(21), 9168–9175; (*f*) A. Ferry, *J. Phys. Chem. B*, 1997, **101**, 150–157; (*g*) A. Ferry, M. M. Doeff and L. C. DeJonghe, *J. Electrochem. Soc.*, 1998, **145**, 1586–1592; (*h*) A. Ferry, G. Orädd and P. Jacobsson, *Electrochim. Acta*, 1998, **43**(10–11), 1471–1476; (*i*) A. Ferry, L. Edman, M. Forsyth, D. R. MacFarlane and J. Sun, *J. Appl. Phys.*, 1999, **86**(4), 2346–2348; (*j*) L. Edman, A. Ferry and P. Jacobsson, *Macromolecules*, 1999, **32**, 4130–4133.

14 (*a*) J. R. Stevens and S. Shantz, *Polym. Commun.*, 1988, **29**, 330–331; (*b*) S. Shantz, J. Sandahl, L. Börjesson, L. M. Torell and J. R. Stevens, *Solid State Ionics*, 1988, **28–30**, 1047–1053; (*c*) M. Kakihana, S. Schantz and L. M. Torell, *J. Chem. Phys.*, 1990, **92**(10), 6271–6277; (*d*) M. Kakihana, S. Schantz, L. M. Torell and J. R. Stevens, *Solid State Ionics*, 1990, **40–41**, 641–644; (*e*) S. Shantz, L. M. Torell and J. R. Stevens, *J. Chem. Phys.*, 1991, **94**(10), 6862–6867.

15 X. Q. Yang, H. S. Lee, L. Hanson, J. McBreen and Y. Okamoto, *J. Power Sources*, 1995, **54**, 198–204.

16 S. F. Johnston, I. M. Ward, J. Cruickshank and G. R. Davies, *Solid State Ionics*, 1996, **90**, 39–48.

17 H. Ericson, B. Mattson, L. M. Torell, H. Rinne and F. Sundholm, *Electrochim. Acta*, 1998, **43**(10–11), 1401–1405.

18 (*a*) L. M. Torell, P. Jacobsson and G. Petersen, *Polym. Adv. Technol.*, 1992, **4**, 152–163; (*b*) G. Petersen, L. M. Torell, S. Panero, B. Scrosati, C. J. Silva and M. J. Smith, *Solid State Ionics*, 1993, **60**, 55–60.

19 (*a*) A. Brodin, B. Mattson, K. Nilsson, L. M. Torell and J. Hamara, *Solid State Ionics*, 1996, **85**, 111–120; (*b*) G. Petersen, A. Brodin, L. M. Torell and M. J. Smith, *Solid State Ionics*, 1994, **72**, 165–171; (*c*) A. Brodin, B. Mattsson and L. M. Torell, *J. Chem. Phys.*, 1994, **101**(6), 4621–4627.

20 (*a*) A. Bernson and J. Lindgren, *Solid State Ionics*, 1993, **60**, 31–36; (*b*) A. Bernson, J. Lindgren, W. Huang and R. Frech, *Polymer*, 1995, **36**(23), 4471–4478; (*c*) A. Bernson and J. Lindgren, *Solid State Ionics*, 1993, **60**, 37–41.

21 S. P. Gejji, K. Hermansson, J. Tegenfeldt and J. Lindgren, *J. Phys. Chem.*, 1993, **97**, 11 402–11 407.

22 (*a*) I. Noda, *J. Am. Chem. Soc.*, 1989, **111**(21), 8116–8118; (*b*) I. Noda, *Appl. Spectrosc.*, 1990, **44**(4), 550–561; (*c*) I. Noda, A. E. Dowrey, C. Marcott, G. M. Story and Y. Ozaki, *Appl. Spectrosc.*, 2000, **54**(7), 236–248.

